Inorg. Chem. **2007**, *46*, 10819–10826

Stoichiometry and Structure of Uranyl(VI) Hydroxo Dimer and Trimer Complexes in Aqueous Solution

Satoru Tsushima,* André Rossberg, Atsushi Ikeda, Katharina Müller, and Andreas C. Scheinost

Institut für Radiochemie, Forschungszentrum Dresden-Rossendorf (FZD), Bautzner Landstraβe 128, D-01328, Dresden, Germany

Received August 13, 2007

We studied the structure and stoichiometry of aqueous uranyl(VI) hydroxo dimers and trimers by spectroscopic (EXAFS, FTIR, UV–vis) and quantum chemical (DFT) methods. FTIR and UV–vis spectroscopy were used for the speciation of uranyl complexes in aqueous solution. DFT calculations show that $(UO_2)_2(OH)_2^{2+}$ has two bridging hydroxo groups with a U–U distance of 3.875 Å. This result is in good agreement with EXAFS, where a U–U distance of 3.88 Å was found. For the hydroxo trimer complex, DFT calculations show that the species $(UO_2)_3(O)(OH)_3^{+}$ with oxo bridging in the center is energetically favored in comparison to its stoichiometric equivalent $(UO_2)_3(OH)_5^{+}$. This is again in line with the EXAFS result, where a shorter U–U distance of 3.81–3.82 Å and evidence for oxo bridging in the center were found. Several stable intermediates which lie several tens of kJ/mol above that of $(UO_2)_3(O)(OH)_3^{+}$ were identified, and their structures, energies, and intramolecular proton-transfer reaction are discussed.

Introduction

The solubility and the speciation of uranium(VI) in water at pH 3−5 with modest (mM to μM) uranium concentrations are dominated by polymeric hydroxo species such as dimeric $(UO_2)_2(OH)_2^{2+}$ or trimeric $(UO_2)_3(OH)_5^{+}$. Peer-reviewed thermodynamic data of various uranyl(VI) polymeric species are available in the OECD/NEA database.[1] However, there are a number of coexisting polymeric hydroxo species with low concentrations in this pH and uranium concentration range, leaving substantial uncertainties on the hydrolysis products. This gap may be overcome by applying direct speciation tools like spectroscopic methods, including vibrational spectroscopy (IR and Raman), UV−vis absorption spectroscopy, and extended X-ray absorption fine structure (EXAFS) spectroscopy.

Nguyen-Trung et al.[2] investigated with Raman spectroscopy a wide concentration and pH range of uranyl(VI) solutions ($0.0038\ \text{M} < \sum U_{conc} < 0.647\ \text{M}$, $0.24 < \text{pH} < 14.96$) by making use of the O═U═O symmetric stretching vibrational frequency (ν_1) of polymeric $(UO_2)_2(OH)^{3+}$, $(UO_2)_2(OH)_2^{2+}$, $(UO_2)_3(OH)_5^{+}$, $(UO_2)_3(OH)_7^{-}$, $(UO_2)_3(OH)_8^{2-}$, $(UO_2)_3(OH)_{10}^{4-}$, and $(UO_2)_3(OH)_{11}^{5-}$. From the observed Raman frequencies, they proposed the structures of four uranyl(VI) trimeric complexes. The ν_1 frequencies provide information on the strength of the O═U═O axial bond, which may then be used to elucidate the equatorial environment such as the type of coordinating ligand and the coordination number. In polymeric species, however, some of the ligands are shared by more than one uranyl unit, and the coordination number around each uranyl unit is not well defined, potentially leading to ambiguous results. Nguyen-Trung et al. proposed a linear correlation between the O═U═O ν_1 frequency (cm^{-1}) and the number of ligands per uranyl unit.[2,3] Such a rule may hold for monomeric species having a constant coordination number of 5, but does not apply for cases where the coordination number is reduced like that in tetrahydroxo $UO_2(OH)_4^{2-}$,[4−5] is increased like that in tricarbonato $UO_2(CO_3)_3^{4-}$,[6−7] where the coordination mode changes from unidentate like in $UO_2(SO_4)^0$ to biden-

* To whom correspondence should be addressed. E-mail: S.Tsushima@fzd.de.

(1) (a) Grenthe, I.; Fuger, J.; Konigs, R. J. M.; Lemire, R. J.; Muller, A. B.; Nguyen-Trung, C.; Wanner, H. *Chemical Thermodynamics of Uranium*; Elsevier Science: New York, 1992; Vol. 1. (b) Guillaumont, R.; Fanghänel, T.; Fuger, J.; Grenthe, I.; Neck, V.; Palmer, D. A.; Rand, M. H. *Update on the Chemical Thermodynamics of Uranium, Neptunium, Plutonium, Americium and Technetium*; Elsevier Science: New York, 2003; Vol. 5.

(2) Nguyen-Trung, C.; Palmer, D. A.; Begun, G. M.; Peiffert, C.; Mesmer, R. E. *J. Solution Chem.* **2000**, *29*, 101.

(3) Nguyen-Trung, C.; Begun, G. M.; Palmer, D. A. *Inorg. Chem.* **1992**, *31*, 5280.

(4) Wahlgren, U.; Moll, H.; Grenthe, I.; Schimmelpfennig, B.; Maron, L.; Vallet, V.; Gropen, O. *J. Phys. Chem. A* **1999**, *103*, 8257.

(5) Moll, H.; Reich, T.; Szabó, Z. *Radiochim. Acta* **2000**, *88*, 411.

10.1021/ic701607e CCC: $37.00
Published on Web 11/10/2007

tate like in $UO_2(SO_4)_2^{2-}$,[8] or when there is an oxo bridging among uranyl moieties, as in the trimeric hydroxo complex $(UO_2)_3(O)(OH)_3^+$.

UV−vis absorption spectroscopy is also a quite useful method for studying the structures of uranyl(VI) complexes because the spectrum reflects structural features, that is, uranyl bond length, coordination number, and the symmetry of the molecule. Polymeric uranyl(VI) species show much-stronger absorption in the visible region (400−450 nm) than that of monomeric species: the molar absorption coefficients of $(UO_2)_2(OH)_2^{2+}$ and $(UO_2)_3(OH)_5^+$ are about 10 and 50 times larger than that of UO_2^{2+}, respectively.[9] When normalized to absorption per uranium atom, $(UO_2)_2(OH)_2^{2+}$ and $(UO_2)_3(OH)_5^+$ still have about 5 and 16 times higher absorption coefficients than UO_2^{2+}. The absorption band is due to the electronic transition from the σ_u HOMO (highest occupied molecular orbital) to the δ_u or ϕ_u LUMO (lowest unoccupied molecular orbital).[10] Both the HOMO and LUMO have mainly 5f character, therefore the observed f−f transition is Laporte forbidden. This selection rule is relaxed, however, when the symmetry is broken, hence the absorption in the visible region shows typical vibronic features (for example, ref 11). Uranyl(VI) polymeric species have high absorption coefficients, whereas their spectra lack fine structural features, suggesting that their symmetry is reduced as compared to the monomer structures, that is, by a bending of the linear O═U═O unit or by the formation of a central oxo bridge in the case of $(UO_2)_3(O)(OH)_3^+$. Furthermore, the absorption maximum shows a red-shift upon polymerization,[9] which suggests a weakening of the uranyl bond (O═U═O), in line with Raman and FTIR data.[12] However, further structural information cannot be deduced solely from the UV−vis spectra.

EXAFS spectroscopy is a more direct way of exploring uranyl(VI) complexes because it provides radial structure information. Moll et al. made the first EXAFS measurements of the uranyl hydroxo trimer $(UO_2)_3(OH)_5^+$ and observed a U−U distance of 3.80 Å.[5] It has been discussed in an earlier review[1] that the complex that is often described as $(UO_2)_3(OH)_5^+$ may be in fact $(UO_2)_3(O)(OH)_3^+$. This point was not discussed in the EXAFS structural investigation by Moll et al.,[5] and this is one of the purposes for revisiting this system. In the present article, EXAFS spectroscopy in combination with density functional theory (DFT) calculations is used to explore the structure of the uranyl(VI) dimer $(UO_2)_2(OH)_2^{2+}$, and the trimer $(UO_2)_3(OH)_5^+$ in aqueous solution. EXAFS spectroscopy can provide U−U distances and U−U coordination numbers, that is, direct proofs for the presence of dimeric or trimeric complexes. The limitation of EXAFS is, however, a limited distal resolution and a general lack of angular information, except in cases where multiple scattering paths can be reliably fitted. This limitation may be overcome by combining EXAFS with DFT, which may be used to calculate the structures of various isomers including hypothetical ones. The limitation of DFT calculations is the accuracy of the obtained energy, which is at best ±10 kJ/mol, hence it is often not possible to find a unique solution for the most-stable geometry of a set of isomers. DFT calculations in combination with CPCM solvation models, however, have provided relatively accurate geometries of aqueous uranyl(VI) complexes.[7−8,13−14] Uranium-to-ligand interatomic distances obtained by DFT and by EXAFS commonly agree within ±0.03 Å.[7,8]

DFT can serve as a tool to correlate thermodynamic speciation and the species obtained by EXAFS. For example, the species $(UO_2)_3(OH)_5^+$ and $(UO_2)_3(O)(OH)_3^+$ are indistinguishable by potentiometric titration because both result in a loss of five protons.[15] However, they should differ significantly in U−U distances, hence they might be distinguished with EXAFS, provided additional structural information is available from DFT. Certainly, only the combination of several techniques can solve the aqueous speciation of such complex systems.

In this work, we applied both B3LYP hybrid density functional theory (DFT) calculations and EXAFS spectroscopy to solve the structures of uranyl(VI) hydroxo dimer and trimer complexes in aqueous solution. One of the main challenges for EXAFS is to prepare solutions in which the target polymeric species are dominant, whereas in the uranium concentration range suitable for EXAFS measurements, there is always a mixing of several species. Therefore, uranium(VI) concentration and pH was optimized as far as possible on the basis of thermodynamic calculations to reduce the number of coexisting species, whereas vibrational spectroscopy (FTIR) and UV−vis absorption spectroscopy were used to support the discrimination of coexisting species, in case they could not be avoided experimentally.

Methods

Materials. All of the sample solutions were prepared from appropriate amounts of $UO_2(NO_3)_2 \cdot 6H_2O$ and tetramethylammonium hydroxide (TMA-OH). TMA-OH was used for pH adjustments. The uranium concentration in solution was determined by ICP−MS. Uranium and TMA-OH concentrations and the pH of the samples are given in Table 1. The preliminary uranyl(VI) speciation as determined by FTIR measurements is also given. Sample solutions with a pH greater than 4.0 were prepared and stored in a glove box under N_2 atmosphere to avoid the formation of carbonate complexes.

FTIR and UV−vis spectroscopy. FTIR and UV−vis spectroscopy were used to estimate the speciation of aqueous uranium(VI). Attenuated total reflectance Fourier-transform infrared (ATR-

(6) Docrat, T. I.; Mosselmans, J. F. W.; Charnock, J. M.; Whiteley, M. W.; Collison, D.; Livens, F. R.; Jones, C.; Edmiston, M. J. *Inorg. Chem.* **1999**, *38*, 1879.
(7) Ikeda, A.; Hennig, C.; Tsushima, S.; Takao, K.; Ikeda, Y.; Scheinost, A. C.; Bernhard, G. *Inorg. Chem.* **2007**, *46*, 4212.
(8) Hennig, C.; Schmeide, K.; Brendler, V.; Moll, H.; Tsushima, S.; Scheinost, A. C. *Inorg. Chem.* **2007**, *46*, 5882.
(9) Meinrath, G. *J. Radioanal. Nucl. Chem.* **1997**, *224*, 119.
(10) Denning, R. *J. Phys. Chem. A* **2007**, *111*, 4125.
(11) Servaes, K.; Hennig, C.; van Deun, R.; Gorller-Walrand, C. *Inorg. Chem.* **2005**, *44*, 7705.
(12) Quilès, F.; Burneau, A. *Vib. Spectrosc.* **2000**, *23*, 231.
(13) Gutowski, K. E.; Dixon, D. A. *J. Phys. Chem. A* **2006**, *110*, 8840.
(14) Shamov, G.A.; Schreckenbach, G. *J. Phys. Chem. A* **2005**, *109*, 10961.
(15) Clark, D. L.; Conradson, S. D.; Donohoe, R.; Keogh, D. W.; Morris, D. E.; Palmer, P. D.; Rogers, R. D.; Tait, C. D. *Inorg. Chem.* **1999**, *38*, 1456.

Table 1. Samples Used in This Study

ID	chemical composition	uranium concentration[a]	pH[a]	speciation[b]
P1	$UO_2(NO_3)_2$ in 0.39 M TMA−OH	534 mM	2.98	**Di**
P2	$UO_2(NO_3)_2$ in 50 mM TMA−OH	47 mM	4.04	**Tri** + **Di** (+Mo)
P3	$UO_2(NO_3)_2$ in 5 mM TMA−OH	17 mM	3.96	**Tri** + **Di** + **Mo**
P4	$UO_2(NO_3)_2$ in 5 mM TMA−OH	4 mM	4.22	**Tri** (+Mo)

[a] Uranium concentration and pH were determined after EXAFS measurements. [b] A rough estimate from FTIR spectra. Mo = monomer, Di = dimer, Tri = trimer. The letter in bold denotes that it is a major species.

FTIR) spectra of aqueous uranyl(VI) solutions were collected between 4000 and 400 cm^{-1} on a Bruker Vertex 80/v vacuum spectrometer equipped with a mercury cadmium telluride detector. Spectral resolution was 4 cm^{-1} and spectra were averaged from 256 scans. The used ATR accessory DURA SamplIR II (Smiths) is a horizontal diamond crystal with nine internal reflections on the upper surface and an angle of incidence of 45°. An ATR flow cell was used for adequate subtraction of the background spectrum. Such a cell allows an exchange of the sample solution without any interference of external thermal perturbations of the equilibrated system, which was found to be essential for the detection of low absorption changes. UV−vis absorption spectra were recorded using a Cary 5G (Varian, Inc.).

EXAFS Spectroscopy. The EXAFS measurements were recorded at the Rossendorf Beamline at BM20 of the European Synchrotron Radiation Facility in Grenoble (France).[16] The Uranium L_{III}-edge spectrum of sample *P*1 (Table 1) was recorded in the fluorescence mode at room temperature, whereas samples *P*2, *P*3, and *P*4 were recorded in the transmission mode. The energy scale was calibrated using the maximum of the first derivative of the K-edge spectrum of yttrium (17 038 eV), which was simultaneously measured with each spectrum. The threshold energy, E_0, of the uranium L_{III} edge was defined as 17 185 eV. The EXAFS spectra were analyzed according to standard procedures using *EXAFSPAK*,[17] including statistical weighting of the 13 fluorescence channels and dead-time correction. Theoretical scattering phases and amplitude functions were calculated with the ab initio calculation program *FEFF8*[18] using the structure of the most-stable form of the trimer complex (Figure 2, C1).

Quantum Chemical Calculations. All of the calculations were performed using *Gaussian 03*.[19] Structures were optimized in the aqueous phase at the B3LYP level by using the CPCM solvation model[20] with UAHF[21] radii. The energy-consistent small-core effective core potential (ECP) and the corresponding basis set suggested by Dolg et al. were used for uranium[22] and oxygen.[23] Moreover, the most diffuse basis functions on uranium with the exponent 0.005 (all s-, p-, d-, and f-type functions) were omitted which made the convergence of the electronic wave function much faster, but had only little effect (less than 1 kJ/mol) on the total energy.[24] For hydrogen, we used the 5s functions contracted to 3s.[25] The Gibbs energy correction to the electronic energy was calculated at the B3LYP level from the vibrational energy levels in aqueous phase and the molecular partition functions. The transition-state search was made in the aqueous phase using *Gaussian 03*, and the transition state was identified through a single imaginary frequency that describes the translation movement across the energy barrier.

Results and Discussions

DFT Structure of the Uranyl(VI) Hydroxo Dimer Complex. Early crystal structure studies by Åberg suggest that the hydroxo dimer complex $(UO_2)_2(OH)_2^{2+}$ has two uranyl units connected via two OH bridges.[26−27]

The DFT calculations on $(UO_2)_2(OH)_2^{2+}$ in the present study were performed by assuming that each uranyl unit has five oxygens in the equatorial plane. Part (a) of Figure 1 shows the structure of $(UO_2)_2(OH)_2(OH_2)_6^{2+}$ optimized in the aqueous phase at the B3LYP level. The U−U distance is 3.875 Å, and the O═U═O angle is 175 degrees. These values disagree with our previous DFT calculations[28] where U−U distances of 3.98−4.09 Å and O═U═O angles of 169−171° were found. The discrepancy may be mainly due to the differences between the optimization in the gas phase and in the solvent and partly due to the difference in the ECPs (small-core ECP in the present study versus large-core ECP in the previous work).

Toth et al.[29] and Fujii et al.[30] identified $(UO_2)_2(OH)_2^{2+}$ in aqueous solution by Raman spectroscopy. It is not possible to obtain a pure $(UO_2)_2(OH)_2^{2+}$ solution because of its thermodynamic equilibrium with UO_2^{2+} and other hydroxo species. Fujii et al.[30] made a careful investigation on the Raman intensity of the O═U═O symmetric stretching vibration (υ_1) of $(UO_2)_2(OH)_2^{2+}$ and concluded that the O═U═O in $(UO_2)_2(OH)_2^{2+}$ is slightly bent. This result was confirmed later by our DFT calculations[28] where an O═U═O angle of ∼170° was determined for $(UO_2)_2(OH)_2(OH_2)_6^{2+}$. To study the stability of $(UO_2)_2(OH)_2^{2+}$ in aqueous

(16) Matz, W.; Schell, N.; Bernhard, G.; Prokert, F.; Reich, T.; Claussner, J.; Oehme, W.; Schlenk, R.; Dienel, S.; Funke, H.; Eichhorn, F.; Betzl, M.; Prohl, D.; Strauch, U.; Huttig, G.; Krug, H.; Neumann, W.; Brendler, V.; Reichel, P.; Denecke, M. A.; Nitsche, H. *J. Synchrotron Rad*. **1999**, *6*, 1076.

(17) George, G. N.; Pickering, I. J. *EXAFSPAK: A Suite of Computer Programs for Analysis of X-ray Absorption Spectra*; Stanford Synchrotron Radiation Laboratory: Stanford, CA. U.S.A., 1995.

(18) Ankudinov, A. L.; Ravel, B.; Rehr, J. J.; Conradson, S. D. *Phys. Rev. B* **1998**, *58*, 7565.

(19) Frisch, M. J.; Trucks, G. W.; Schlegel, H. B.; Scuseria, G. E.; Robb, M. A.; Cheeseman, J. R.; Montgomery, J. A., Jr.; Vreven, T.; Kudin, K. N.; Burant, J. C.; Millam, J. M.; Iyengar, S. S.; Tomasi, J.; Barone, V.; Mennucci, B.; Cossi, M.; Scalmani, G.; Rega, N.; Petersson, G. A.; Nakatsuji, H.; Hada, M.; Ehara, M.; Toyota, K.; Fukuda, R.; Hasegawa, J.; Ishida, M.; Nakajima, T.; Honda, Y.; Kitao, O.; Nakai, H.; Klene, M.; Li, X.; Knox, J. E.; Hratchian, H. P.; Cross, J. B.; Bakken, V.; Adamo, C.; Jaramillo, J.; Gomperts, R.; Stratmann, R. E.; Yazyev, O.; Austin, A. J.; Cammi, R.; Pomelli, C.; Ochterski, J. W.; Ayala, P. Y.; Morokuma, K.; Voth, G. A.; Salvador, P.; Dannenberg, J. J.; Zakrzewski, V. G.; Dapprich, S.; Daniels, A. D.; Strain, M. C.; Farkas, O.; Malick, D. K.; Rabuck, A. D.; Raghavachari, K.; Foresman, J. B.; Ortiz, J. V.; Cui, Q.; Baboul, A. G.; Clifford, S.; Cioslowski, J.; Stefanov, B. B.; Liu, G.; Liashenko, A.; Piskorz, P.; Komaromi, I.; Martin, R. L.; Fox, D. J.; Keith, T.; Al-Laham, M. A.; Peng, C. Y.; Nanayakkara, A.; Challacombe, M.; Gill, P. M. W.; Johnson, B.; Chen, W.; Wong, M. W.; Gonzalez, C.; Pople, J. A. *Gaussian 03*, revision D.01; Gaussian, Inc.: Wallingford, CT, 2004.

(20) Barone, V.; Cossi, M. *J. Phys. Chem A* **1998**, *102*, 1995−2001.

(21) Bondi, A. *J. Phys. Chem*. **1964**, *68*, 441−451.

(22) Küchle, W.; Dolg, M.; Stoll, H.; Preuss, H. *J. Chem. Phys*. **1994**, *100*, 7535.

(23) Bergner, A.; Dolg, M.; Kuechle, W.; Stoll, H.; Preuss, H. *Mol. Phys*. **1993**, 80, 1431.

(24) Macak, P.; Tsushima, S.; Grenthe, I.; Wahlgren, U. *Dalton Trans.* **2006**, 3638.

(25) Krishnan, R.; Binkley, J. S.; Seeger, R.; Pople, J. A. *J. Chem. Phys*. **1980**, *72*, 650.

(26) Åberg, M. *Acta Chem. Scand.* **1969**, *23*, 791.

(27) Åberg, M. *Acta Chem. Scand.* **1970**, *24*, 2901.

(28) Tsushima, S.: Reich, T. *Chem. Phys. Lett*. **2001**, *347*, 127.

(29) Toth, L. M.; Begun, G. M. *J. Phys. Chem*. **1981**, *85*, 547.

(30) Fujii, T.; Fujiwara, K.; Yamana, H.; Moriyama, H. *J. Alloys Compd.* **2001**, *323*−*324*, 859.

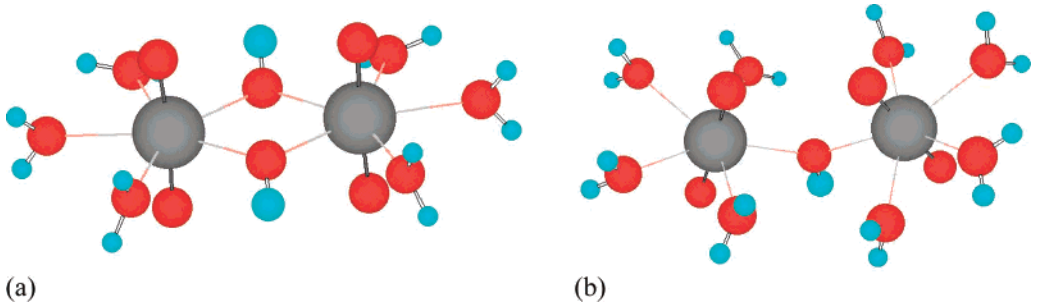

Figure 1. Geometries of (a) $(UO_2)_2(OH)_2(OH_2)_6^{2+}$ and (b) $(UO_2)_2(OH)(OH_2)_8^{3+}$ optimized in the aqueous phase at the B3LYP level. The U−U distances are 3.875 Å for (a), and 4.390 Å for (b).

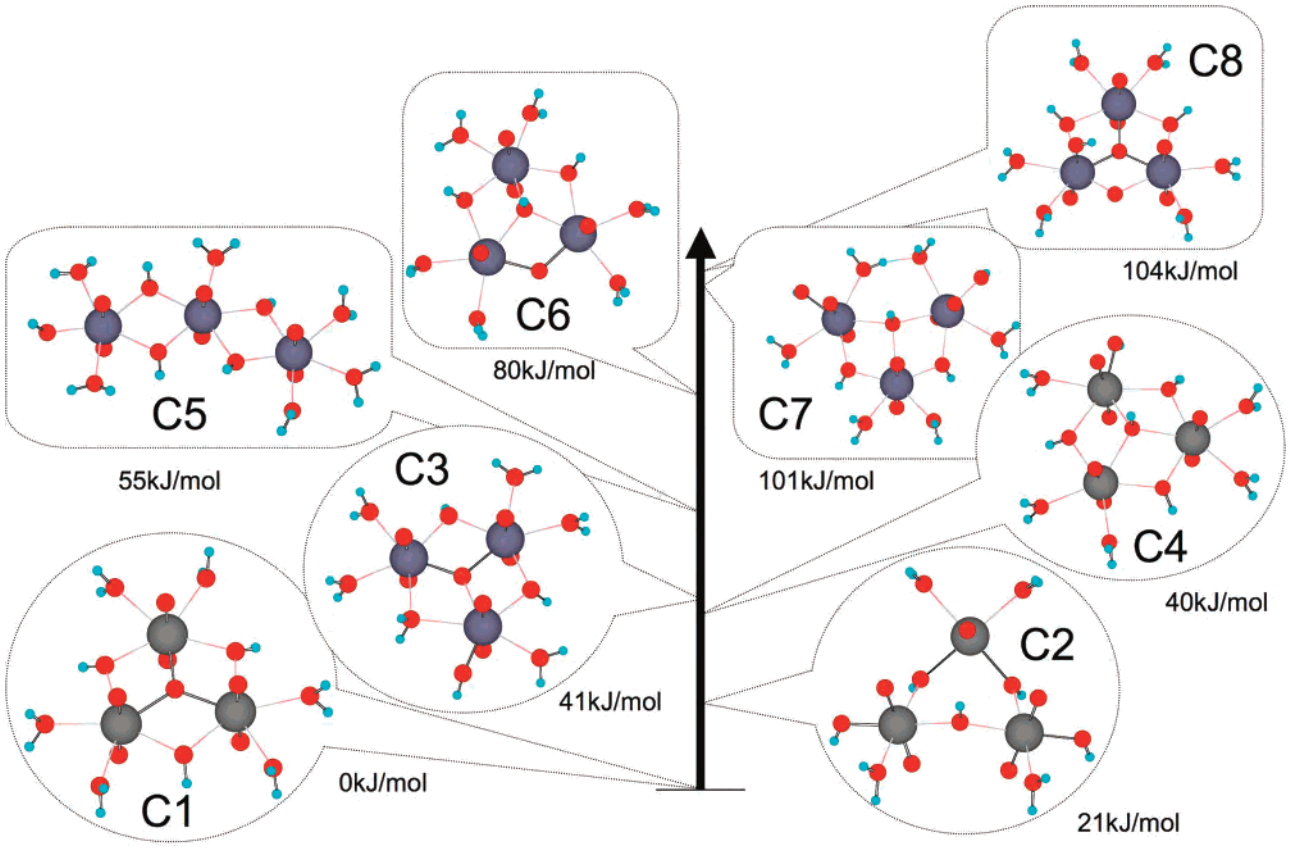

Figure 2. Structures and relative Gibbs energies of various isomers of $(UO_2)_3(OH)_5^+$ and its stoichiometric equivalent $(UO_2)_3(O)(OH)_3^+$ as obtained by B3LYP calculations. C1 was found to be the most-stable geometry.

solution, Oda et al.[31] performed DFT calculations and compared the binding energies of $(UO_2)_2(OH_2)_8^{4+}$ and $(UO_2)_2(OH)_2(OH_2)_6^{2+}$. They concluded that the OH bridging in $(UO_2)_2(OH)_2(OH_2)_6^{2+}$ is more stable than the water bridging in $(UO_2)_2(OH_2)_8^{4+}$. However, it is not appropriate to use the binding energies to compare the stability of these two complexes because the formation of $(UO_2)_2(OH_2)_8^{4+}$ involves only the loss of water molecules, whereas the formation of $(UO_2)_2(OH)_2(OH_2)_6^{2+}$ involves the loss of water and protons, thus being dependent on pH. Despite the fact that Oda et al. did not adequately take into account the pH dependency of the speciation, their conclusion is still valid because the formation of water-bridged $(UO_2)_2(OH_2)_8^{4+}$ is a large endothermic reaction, and this species cannot emerge under ambient temperature. In other words, the OH-bridged species is more stable than the water-bridged species at any pH.

We also performed the structure optimization of $(UO_2)_2OH^{3+}$ a uranyl hydroxo dimer with single OH bridging. To our knowledge, the structure of this complex in solution is not well characterized except that the O═U═O symmetric stretching vibrational frequency (υ_1) has been identified at 860 cm^{-1}.[2] The DFT calculation of $(UO_2)_2(OH)(OH_2)_8^{3+}$ provided the optimal geometry shown in part (b) of Figure 1. This structure has a relatively long U−U distance of 4.390 Å with a U−O−U angle of 140°. The structure is very similar to that of $(UO_2)_2F(OH_2)_9^{3+}$, which is an intermediate state of a fluoride-exchange reaction between UO_2^{2+} and UO_2F^+.[24] This fluoride-exchange intermediate, $(UO_2)_2F(OH_2)_9^{3+}$, is known to stay only 13 kJ/mol above the precursor complex. Because of its short kinetic lifetime, however, it is not possible to observe $(UO_2)_2F^{3+}$ in aqueous

(31) Oda, Y.; Aoshima, A. *J. Nucl. Sci. Technol.* **2002**, *39*, 647.

solution. Compared to a weakly bound fluoride ligand, OH^- can form much-stronger bridging between two uranyl(VI) units, and the corresponding complex $(UO_2)_2(OH)^{3+}$ may exist in solution at a detectable level. Thermodynamic speciation calculations indicate that this species can become dominant when the total uranyl(VI) concentration in solution exceeds several 100 mM at around pH 3. The Raman spectroscopic study by Nguyen-Trung et al.[2] also confirms this idea.

DFT Structures and Dynamics of Uranyl(VI) Hydroxo Trimer Complexes. Various possible isomers were considered in the DFT calculations. Figure 2 shows optimized structures and relative energies of major models that were considered. All of the structures were optimized in the aqueous phase at the B3LYP level, and the energy here is the relative Gibbs energy in the aqueous phase. To make all of the models stoichiometrically comparable, the Gibbs energy of a water molecule calculated at the same level of theory was added to the Gibbs energy of some of the models. This approach suffers from two disadvantages. First, the solvation sphere is counted twice if one simply adds the Gibbs energy of two independent complexes. Second, the basis set superposition error may be different for the two models. To get around this problem, one may add additional water molecules in the second hydration sphere to make the number of atoms consistent in all of the models. As Tsushima recently pointed out,[32] this is also not a feasible way because this type of an ill-shaped model tends to overestimate the energetic stability of the complex and because no stable position for the additional water molecules in the second hydration sphere could be derived. Therefore, we decided to add the energy of two separate complexes in spite of the above-mentioned dilemma.

In Figure 2, complex C1 was found to have the most-stable geometry. This complex has the stoichiometry $(UO_2)_3(O)(OH)_3(H_2O)_6^+$ with an oxo bridge in the center. $(UO_2)_3(O)(OH)_3^+$ and $(UO_2)_3(OH)_5^+$ are indistinguishable by potentiometric titration because both result in a loss of five protons. Hence, the thermodynamic data obtained for $(UO_2)_3(OH)_5^+$ could actually be that of $(UO_2)_3(O)(OH)_3^+$. In the OECD/NEA review of uranium thermodynamic data, this point has been discussed in detail (page 108 in ref 1a), and because no final conclusion could be drawn, both oxo-centered species and hydroxo-centered species have to be considered here. The structure of complex C1 obtained by DFT calculation is very similar to that of solid $[(UO_2)_3(O)(OH)_3(H_2O)_6]NO_3{\cdot}4H_2O$ identified by Åberg.[33] In complex C1 (and in $[(UO_2)_3(O)(OH)_3(H_2O)_6]NO_3{\cdot}4H_2O$), the average distances are 3.834 Å (3.81 Å) for U−U, 1.788 Å (1.78 Å) for $U-O_{ax}$, 2.214 Å (2.21 Å) for $U-O_{center}$, 2.542 Å (2.45 Å) for $U-O_{water}$, and 2.391 Å (2.42 Å) for $U-O_{OH}$; hence, all of the distances except for the $U-O_{water}$ distance show very good agreement between the DFT-derived structure of the aqueous complex and the crystal structure of the solid.

We performed a Mulliken population analysis of dimer and trimer complexes to study the nature of the central oxo ligand. The effective charge of oxygen in $(UO_2)_3(O)(OH)_3(H_2O)_6^+$ are −0.40 (O_{ax}), −0.80 (O_{center}), −0.99 (O_{OH}), and −0.93 (O_{water}), whereas in $(UO_2)_2(OH)_2(H_2O)_6^{2+}$ they are −0.32 (O_{ax}), −0.98 (O_{OH}), and −0.94 (O_{water}). Uranium d and f populations in $(UO_2)_3(O)(OH)_3(H_2O)_6^+$ are d 11.72, f 2.43 (f_σ 1.075, f_π 0.973, f_δ 0.114, f_ϕ 0.269), and in $(UO_2)_2(OH)_2(H_2O)_6^{2+}$ they are d 11.69, f 2.43 (f_σ 1.113, f_π 1.031, f_δ 0.062, f_ϕ 0.220). Hence, there is only a small difference in d and f orbital populations between dimer and trimer complexes. Presumably, the central oxo is acting as both a π and a σ donor to uranium, whereas the $U-O_{ax}$ bond is extended when going from the dimer (1.770 Å) to the trimer (1.788 Å) structure, and consequently the uranium 5f and 6d orbital populations remain basically unchanged.

The second most stable structure is C2, with an energy of only 21 kJ/mol above that of C1. Complex C2 has no central bridging, and three uranyl units are connected via three OH groups, that is, each U−U pair is bridged via one OH group. Because of steric effects, a coordination number (CN) of 5 is unlikely; hence, we assumed a CN of 4. This model has U−U distances of 4.31 to 4.42 Å, which are about 0.5−0.6 Å longer than those of the C1 model. The variation in U−U distances (4.31−4.42 Å) comes from the fact that the three uranyl(VI) units are not equivalent.

The next-stable structures are C3 and C4, with energies of about 40 kJ/mol above that of C1. In complex C3, one proton in the coordinating water of C1 moves to the OH bridge to form a water bridge. The proton in the water bridge in C3 may move further to the central oxo ligand to form C4, which is very close in energy to C3.

To study the lability of the proton and to estimate the reaction barrier to form C3, we tried to identify the transition state between C1 and C3. It was not possible to identify the transition state connecting C1 and C3. It was found that the breaking of the OH bridge precedes the proton-transfer reaction. C3 forms from C1 via two intermediate states, which are given in Figure 3. First, one of the three OH bridges is broken to form C11; then, a proton is transferred to form C12. The transition state describing the OH breaking (TS1) and the proton transfer (TS2) was identified. It was not possible to identify the transition state between C12 and C3. However, the reaction barrier to form C3 from C1 via C11 and C12 was found to be low, with an activation Gibbs energy of about 50 kJ/mol. The OH bridges can also break rather easily. An attempt to identify the transition state between C3 and C4 failed.

C4 is a possible intermediate for the central oxo ligand-exchange reaction. Another possible intermediate for the oxo ligand exchange is C6, but C6 is about 40 kJ/mol above C4. This suggests that it is unlikely that the proton can be transferred directly from the OH bridge to the central oxo group. The proton passes more likely through the formation of water-bridged species via a break in the OH bridging, that is, C1 → C3 → C4.

Another possible isomer is complex C5, which has an almost linear U−U−U unit and an energy of 55 kJ/mol above C1. C7 and C8 are other possible isomers, but these

(32) Tsushima, S. *J. Phys. Chem. A* **2007**, *111*, 3613.
(33) Åberg, M. *Acta Chem. Scand. A* **1978**, *32*, 101.

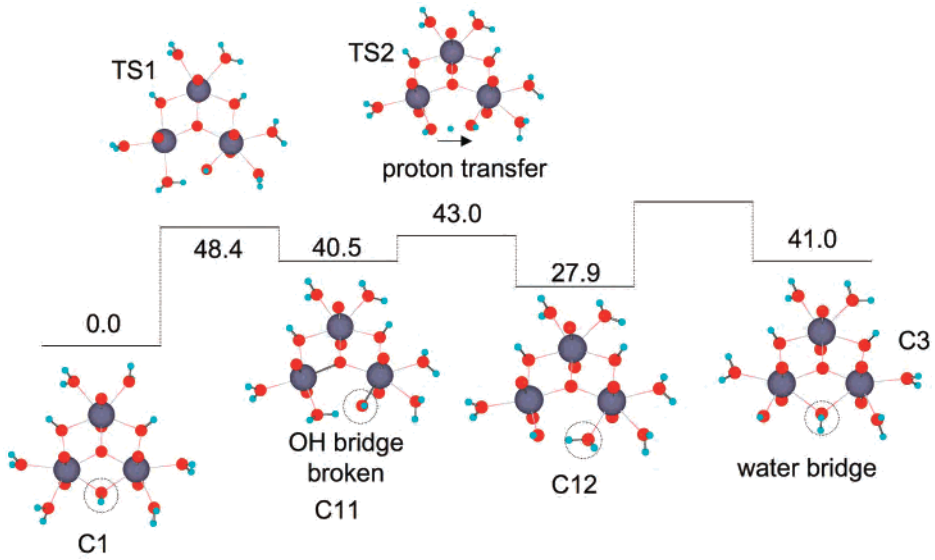

Figure 3. Structures and relative Gibbs energy (kJ/mol) of the precursor, intermediates, and transition states from an OH-bridged precursor to a water-bridged uranyl hydroxo trimer via an intramolecular proton-transfer process.

complexes are much higher in energy; therefore, they may act as intermediate states but not as stable energy minima.

In summary, the DFT calculations reveal that the species $(UO_2)_3(O)(OH)_3^+$ with an oxo central bridging and a U−U distance of 3.834 Å is the most-stable structure of $(UO_2)_3(OH)_5^+$. There are several isomers that are energetically close to this energy minimum. All of the isomers have characteristic U−U distances; therefore, the U−U distance should be a reliable way to identify which isomer actually exists in aqueous medium. We will discuss this point later in the article.

FTIR and UV−Vis Spectroscopy. From the FTIR spectra, we estimated the approximate uranyl(VI) speciation of each sample (Table 1). The FTIR spectra are given as Supporting Information (Figure S1). According to a previous study, the IR active asymmetric stretching vibration of the O═U═O unit has υ_3 vibrational frequencies at 961 cm^{-1}, 943 cm^{-1}, and 923 cm^{-1} for UO_2^{2+}, $(UO_2)_2(OH)_2^{2+}$, and $(UO_2)_3(OH)_5^+$, respectively.[12] All of our spectra have a strong peak at 950 cm^{-1} due to TMA-OH. This peak does not interfere with the asymmetric stretching vibrational frequency (υ_3) of the uranyl unit. Solution P1 has two strong peaks at 950 cm^{-1} and 942 cm^{-1}, and a minor peak at 961 cm^{-1}, suggesting prevalently $(UO_2)_2(OH)_2^{2+}$. Samples P2 and P3 are mixtures of monomeric, dimeric, and trimeric species. P2 has a less-monomeric contribution than P3 and is predominantly a mixture of dimeric and trimeric species. P4 consists mainly of a trimer with only a small fraction of monomer.

The UV−vis absorption spectra were also measured to obtain information about the uranyl(VI) speciation. According to Meinrath,[9] the molar absorption coefficient of the uranyl(VI) f−f transition is lowest in UO_2^{2+} and highest in $(UO_2)_3(OH)_5^+$. Figure S2 shows the absorption spectra of samples P1−P4. Each spectrum is normalized according to the uranium concentration. Sample P2 shows the highest absorption maxima and P1 the lowest. These results are in line with the uranyl(VI) speciation deduced from FTIR.

EXAFS Spectroscopy. The k^3-weighted EXAFS spectra of samples P1−P4 and their corresponding Fourier transforms (FTs) are shown in Figure 4. The obtained structural parameters are given in Table 2. According to the FTIR and UV−vis measurements, samples P1−P4 contain mixtures of UO_2^{2+}, $(UO_2)_2(OH)_2^{2+}$, and $(UO_2)_3(OH)_5^+$. The formation of polynuclear complexes is confirmed by EXAFS for samples P2−P4, which all show U−U backscattering. By shell fitting, we obtained a U−U radial distance of 3.82−3.83 Å, which is in line with the trimer complex $(UO_2)_3(OH)_5^+$ (Table 2, fit model 1). For sample P1, a weak FT peak at 3.71 Å could be fitted by 0.5 uranium atoms at a radial distance of 3.88 Å (Figure 4, Table 2). This distance is in line with the dimeric complex $(UO_2)_2(OH)_2^{2+}$. The U−U distances found here show good agreement with the crystal structure data and the DFT calculations. The averaged U−U distances are 3.875 Å (DFT) versus 3.88 Å (EXAFS) for $(UO_2)_2(OH)_2^{2+}$, and 3.834 Å (DFT) versus 3.81−3.82 Å (EXAFS) for $(UO_2)_3(O)(OH)_3^+$. A shorter U−U distance of 3.81−3.82 Å in the trimeric complex suggests the presence of the central oxo bridging instead of the OH bridging. The special structural arrangement of the three UO_2 units in the most-stable form of the trimer complex (Figure 2, C1) should result in an oxygen shell between 4.32 and 4.35 Å due to backscattering from the four O_{ax} atoms of the two neighboring UO_2 units (Table 2, fit model 2). When fitting this shell ($U-O_{ax(trimer)}$, fit model 1), the F value decreased slightly from $F = 20.7$ to 20.3 (P2), from $F = 20.9$ to 20.6 (P3), and from $F = 22.5$ to 22.4 (P4) (Table 2), thereby supporting the structural model derived from DFT. Including the $U-O_{ax(trimer)}$ scattering contribution did not influence the neighboring U−U distance and coordination number of model 1 (Table 2). In the case of the trimer, it was not possible to fit the O_{eq} shell after adding the expected central oxygen atom at 2.21 Å. A stable fit could be achieved only if at least two additional shells were included. Because of the limited resolution in R space

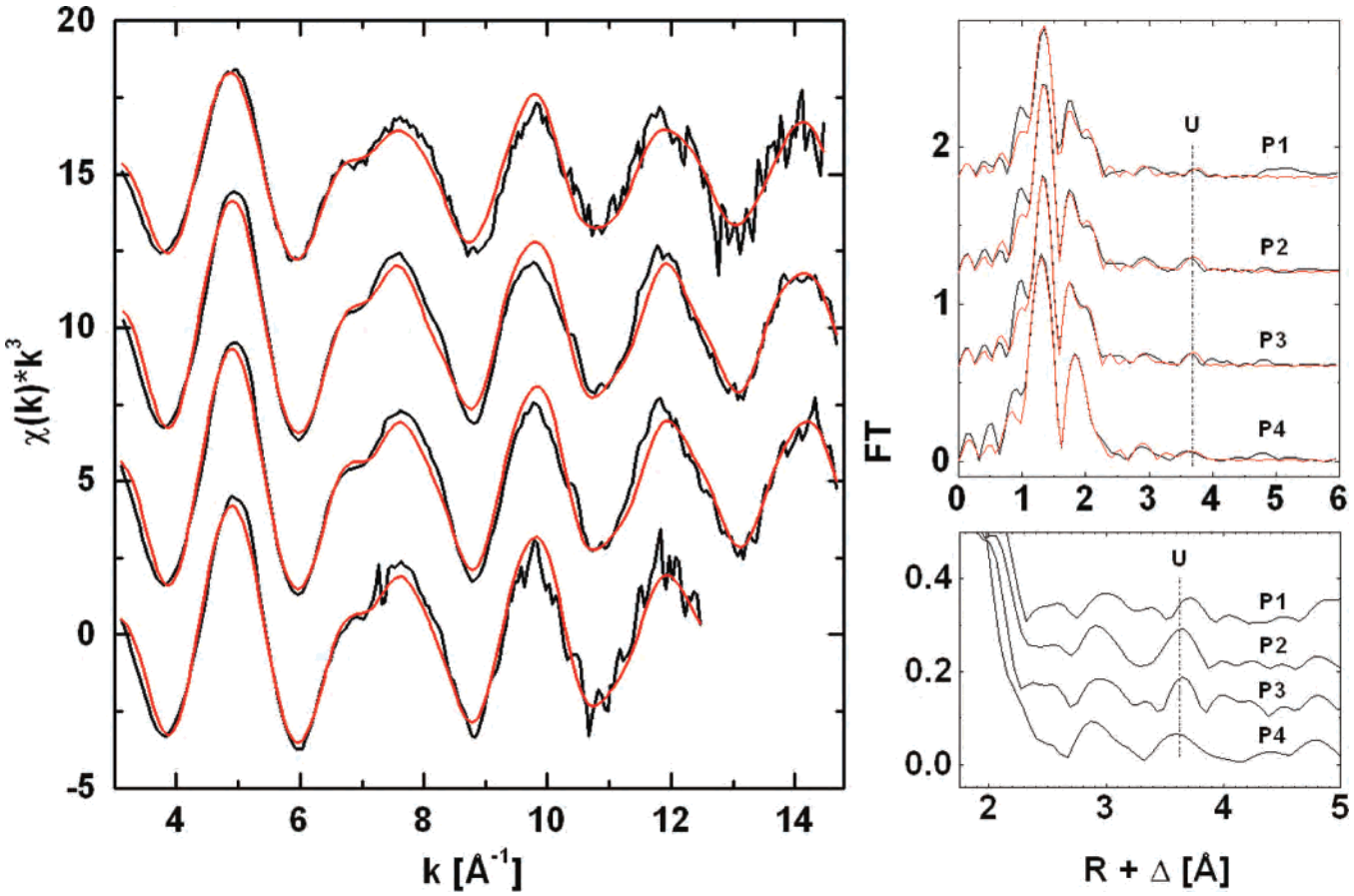

Figure 4. k^3-weighted U−L_{III} edge EXAFS spectra of aqueous hydrolysis species (P1−P4) and corresponding Fourier transforms. Black lines are experimental data, and red lines are the fits. The dashed line marks the uranium backscattering signal.

Table 2. EXAFS Structural Parameters for Sample P1 and for Samples P2−P4 Using Two Different Shell Fit Models

spectrum	shell	CN[a]	R (Å)[b]	σ^2 (Å^2)·10^{3}[c]	ΔE_0 (eV)[d]	F[e]
P1 k: 3.1−14.5 Å^{-1}	U═O	2*	1.770(2)	1.3(1)	−8.8(7)	29.9
	U−O_{eq}	5.0(6)	2.412(7)	10(1)	[i]	
	U−U	0.5(2)	3.88(2)	6[h]	[i]	
P2 k: 3.1−14.7 Å^{-1}	U═O	2*	1.771(1)	1.51(8)	−8.2(5)	20.7[f]
	U−O_{eq}	5.3(5)	2.408(6)	13(1)	/	
	U−U	0.7(1)	3.82(1)	6[h]	/	
	U−U[g]	0.8(2)	3.81(1)	6[h]		20.3[g]
	U−$O_{ax(trimer)}$[g]	2.9(9)	4.30(2)	7[h]		
P3 k: 3.1−14.7 Å^{-1}	U═O	2*	1.766(1)	1.46(8)	−8.6(4)	20.9[f]
	U−O_{eq}	5.3(4)	2.407(5)	10.7(9)	[i]	
	U−U	0.7(2)	3.83(1)	6[h]	[i]	
	U−U[g]	0.8(2)	3.82(1)	6[h]		20.6[g]
	U−$O_{ax(trimer)}$[g]	3(1)	4.34(3)	7[h]		
P4 k: 3.1−12.5 Å^{-1}	U═O	2*	1.769(2)	1.4(1)	−8.2(5)	22.5[f]
	U−O_{eq}	4.6(4)	2.410(5)	10(1)	[i]	
	U−U	0.5(2)	3.83(2)	6[h]	[i]	
	U−U[g]	0.6(2)	3.82(2)	6[h]		22.4[g]
	U-$O_{ax(trimer)}$[g]	2(1)	4.33(6)	7[h]		

[a] Coordination number. [b] Atomic distance. [c] Debye−Waller factor. [d] Energy-shift parameter linked for all paths. [e] F value as estimated by *EXAFSPAK*. [f] Shell fit model 1. [g] Shell fit model 2. [h] Fixed parameter. [i] Linked parameter.

(0.14−0.17 Å), however, we report only average O_{eq} shell parameters like for sample P1.

The U−U coordination numbers of samples P1−P4 are less than 1 and hence too small for dimers and trimers. This is related to the fact that all of the samples were mixtures of monomeric and polymeric species. In addition, the CN obtained from EXAFS always has an error of ∼10−20%. Clearly, the coordination numbers obtained from EXAFS do not help to identify the polymer structures, whereas the U−U distances give reliable results.

In the following, we compared our EXAFS and DFT structures with published crystal structures of uranyl polymeric complexes. In fact, the DFT structure of $(UO_2)_3(O)(OH)_3(H_2O)_6^+$ agrees well with the crystal structure of $[(UO_2)_3(O)(OH)_3(H_2O)_6]NO_3{\cdot}4H_2O$,[33] as discussed already earlier. However, it should also be noted that the U−U

distances may vary with the respective counterions and their spatial distribution. For example, $[(UO_2)_3(O)(OH)_3(H_2O)_6]NO_3 \cdot 4H_2O$ has a U−U distance of 3.809 Å,[33] whereas the uranyl hydroxo polymer with the chlorine counterion has U−U distances of 3.86 Å in the trimer and 3.944 Å in the dimer.[26,27] A comparison with the structure of uranyl trimers without bridging OH ligands[34] or a comparison with the structure of the uranyl tetramer[35] is even more complicated, and therefore we do not refer to these data in the present discussions.

To summarize, the EXAFS spectra of four different uranyl(VI) samples show two distinct U−U distances of 3.88 and ~3.81−3.82 Å, which correspond to $(UO_2)_2(OH)_2^{2+}$ and $(UO_2)_3(O)(OH)_3^{+}$, respectively. These distances agree well with the results of the DFT calculations. Our combined DFT and EXFAS results confirm that $(UO_2)_3(OH)_5^{+}$ in aqueous solution exists as $(UO_2)_3(O)(OH)_3^{+}$ with an oxo central bridging.

Conclusions

We have studied the structures of $(UO_2)_2(OH)_2^{2+}$ and $(UO_2)_3(O)(OH)_3^{+}$ both by DFT calculations and EXAFS spectroscopy. The structures obtained by DFT calculations are in good agreement with EXAFS results and confirm the idea that $(UO_2)_3(O)(OH)_3^{+}$ is more stable than its stoichiometric equivalent $(UO_2)_3(OH)_5^{+}$. Because of the presence of the central oxo bridging, $(UO_2)_3(O)(OH)_3^{+}$ has U−U distances of 3.81−3.82 Å, which are shorter than the U−U distance in $(UO_2)_2(OH)_2^{2+}$ (3.88 Å).

Acknowledgment. We thank Drs. Vinzenz Brendler, Harald Foerstendorf, Henry Moll, and Christoph Hennig for stimulating discussions. We also acknowledge helpful advise from Professor Ingmar Grenthe, of the Royal Institute of Technology (KTH), Sweden, at an early stage of this work. S.T. was supported by the Alexander von Humboldt foundation. A.I. was supported by the Deutsche Forschungsgemeinschaft (DFG) under contract HE 2297/2-1. The authors also acknowledge the generous allocation of computation time on supercomputers at Zentrum für Informationsdienste and Hochleistungsrechnen (ZIH), Technische Universität Dresden, Germany.

Supporting Information Available: FTIR and UV−vis spectra of the samples. Coordinates of all of the precursors, intermediates, and transition states. This material is available free of charge via the Internet at http://pubs.acs.org.

IC701607E

(34) Szabó, Z.; Furó, I.; Csöregh, I. *J. Am. Chem. Soc.* **2005**, *127*, 15236.
(35) Weller, M. T.; Light, M. E.; Gelbrich, T. *Acta Crystallogr. B* **2000**, *56*, 577.